J Mater Sci: Mater Electron (2017) 28:12885–12890
DOI 10.1007/s10854-017-7118-9

Uniform cerium-based metal–organic framework microflowers: controlled synthesis, characterization and formation mechanism

Zhanglei Ning[1] · Xi He[1] · Lin He[1] · Xiting Lei[1] · Yingjiong Lu[1] · Jian Bi[1] · Daojiang Gao[1] · Changyan Sun[2] · Wenjun Li[2]

Received: 14 February 2017 / Accepted: 9 May 2017 / Published online: 13 May 2017

Abstract Three dimensional (3D) flower-like cerium pyrazine-2,3,5,6-tetracarboxylate metal–organic framework has been successfully prepared on a large scale through a simple and facile hydrothermal method without the assistance of any surfactant or template. The composition and structure of the samples were well characterized by Fourier transform infrared spectroscopy, X-ray powder diffraction, elemental analysis, thermogravimetric analysis, scanning electron microscopy, and energy dispersive X-ray, respectively. The experimental results indicate that these 3D flower-like architectures with diameter of about 4 μm are composed of a large number of nanosheets. The presumed molecular formula of the cerium-based metal–organic framework is $Ce_2(pztc)(H_2O)_6$. In addition, a possible mechanism for the formation of cerium pyrazine-2,3,5,6-tetracarboxylate architectures was proposed based on time-dependent experiments. Furthermore, the as-obtained flower-like cerium-based metal–organic framework architectures could be easily transformed into CeO_2 microstructures with flower-like outlines through simply heat-treating in air.

✉ Daojiang Gao
daojianggao@126.com

✉ Wenjun Li
wenjunli_ustb@126.com

[1] College of Chemistry and Materials Science, Sichuan Normal University, Chengdu 610068, China

[2] School of Chemical and Biological Engineering, University of Science and Technology Beijing, Beijing 100083, China

1 Introduction

In recent years, three dimensional (3D) microstructured architectures have been received a great deal of attention in the area of materials science owing to their interesting superstructures and potential applications in sensors, catalysis, and supercapacitors [1, 2]. Up to now, a variety of methods were used to synthesize materials with complex 3D hierarchical superstructures [3, 4]. However, the introduction of catalysts, surfactant, or template for the fabrication of these hierarchical architectures induces heterogeneous impurities, increases the production cost, and leads to difficulty for scale-up production [5]. Thus, it is necessary to develop an easy, rapid, and one step method to produce highly pure, hierarchical architectures to meet the requirements for potential industrialization uses in material science.

Metal–organic frameworks (MOFs), which constructed from metal ions and organic bridging ligands via the self-assembly process, have received more attention not only because of their fascinating architectures but also for extensive applications in high performance magnets, catalysts, luminescence sensors and other functional materials [6–10]. During the past decades, the majority researches of these MOFs materials are focused on the structural study of macro-scaled single crystalline products. With the development of nanoscience and nanotechnology, miniaturizing the size of metal–organic frameworks to nano/micro-scale has gained growing attention [11]. More recently, some synthetic strategies have been developed for the preparation of nano/micro-scaled metal–organic frameworks, such as microwave [12], reverse microemulsion [13], interface reaction [9, 14], and solvothermal methods [15, 16]. These thought-provoking works inspired us to explore a simple and effective approach for preparing nano/micro-scaled

metal–organic materials from the molecular level and controlling the growth process to meet the requirement for potential applications.

In our previous studied, some micro/nano-sized lanthanide-based metal–organic frameworks have been reported [17, 18]. In this paper, cerium pyrazine-2,3,5,6-tetracarboxylate metal–organic frameworks (Ce-MOFs) with uniform 3D flower-like architectures have been successfully prepared through a simple and facile hydrothermal method. A possible mechanism for the formation of cerium pyrazine-2,3,5,6-tetracarboxylate architectures was proposed based on the time-dependent experiments. In addition, the preparation of shape-preserved CeO_2 from the thermal decomposition of Ce-MOFs was also investigated.

2 Experimental section

2.1 Preparation

Pyrazine-2,3,5,6-tetracarboxylic acid (pztc) was synthesized according to the literature with slight modification [19]. In a typical synthesis of cerium pyrazine-2,3,5,6-tetracarboxylate microflowers, 0.0384 g of 2,3,5,6-tetramethylpyrazine were dissolved in 10 mL distilled water system under agitated stirring to get a transparent solution. Then 5 mL of 0.03 M $Ce(NO_3)_3$ solution was added into the solution under stirring. After vigorous stirring for 20 min, 0.35 M KOH was added into the above solution to adjust the pH of the solution to 7. After additional agitation for 30 min, the mixed solution was transferred into a 25 mL Teflon bottle held in a stainless steel autoclave, sealed, and maintained at 120 °C for 24 h. As the autoclave cooled to room temperature naturally, the resulting precipitations were separated by centrifugation, washed several times with water and absolute ethanol, and finally dried under oven at 50 °C. Time-dependent experiments were carried out by adjusting the reaction time (1–48 h) with other fixed reaction parameters.

2.2 Characterization

Fourier transform infrared spectroscopy (FTIR) spectrum was obtained on NEXUS 670 (Thermo Nicolet). The spectrum was recorded in the 4000–400 cm^{-1} region with the resolution of 4 cm^{-1} by using pressed KBr tables. X-ray powder diffraction (XRD) was performed on D/MAX-RB diffractometer (Rigaku) with Cu Kα source in the 2θ range from 5° to 80°. Thermogravimetric analysis (TGA) data were recorded on Q 500 analyzer (TA) with a heating rate of 10° min^{-1} in air. Elemental analysis of C, N and H in the solid samples was carried out on EA 3000 (EuroVector). The morphology was inspected using Quanta 250 (FEI) scanning electron microscope (SEM). The energy dispersive X-ray spectrum (EDX) was measured with Genesis Apex (EDAX).

3 Results and discussion

3.1 Chemical composition and structure of Ce-MOFs

FT-IR spectrum was first used to investigate the chemical composition of the as-obtained cerium pyrazine-2,3,5,6-tetracarboxylate (Ce-MOFs) products. In Fig. 1, the characteristic bands of the nonionized carboxyl group of pyrazine-2,3,5,6-tetracarboxylate disappear (1724 cm^{-1}) [18] and new bands observed at 1606 and 1419 cm^{-1} which are attributed to the asymmetric and symmetric stretching vibration of the ionized carboxyl group. It proves that the Ce^{3+} ions have been coordinated with the pyrazine-2,3,5,6-tetracarboxylate ligands successfully. Furthermore, the broad band peaked at 3402 cm^{-1} should be the –OH stretching vibration of the water groups, indicating that the water molecules exist in the structure of the as-obtained samples [20].

The crystal structure of the products was determined by X-ray powder diffraction (XRD). From Fig. 2, it can be seen that the products of Ce-MOFs were crystallized under this mild reaction conditions. However, on the basis of the JCPDS standard reference database, materials showing such diffraction peaks have been unknown till now. Actually, owing to the complexity of the bonding between metal ion and organic ligand, the reported crystal structures are not abundant and sufficient for the identification of MOFs materials. It has been found that the crystalline MOFs

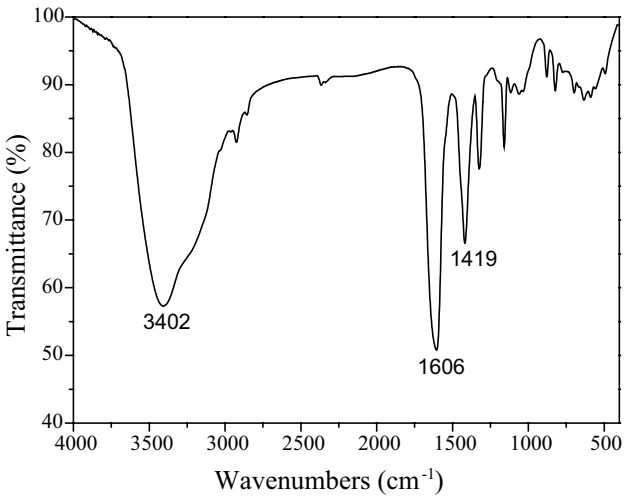

Fig. 1 FT-IR spectrum of the cerium pyrazine-2,3,5,6-tetracarboxylate samples

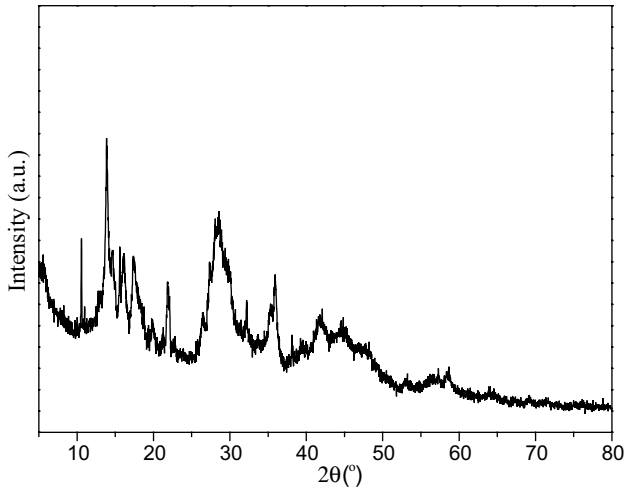

Fig. 2 XRD pattern spectrum of the cerium pyrazine-2,3,5,6-tetracarboxylate samples

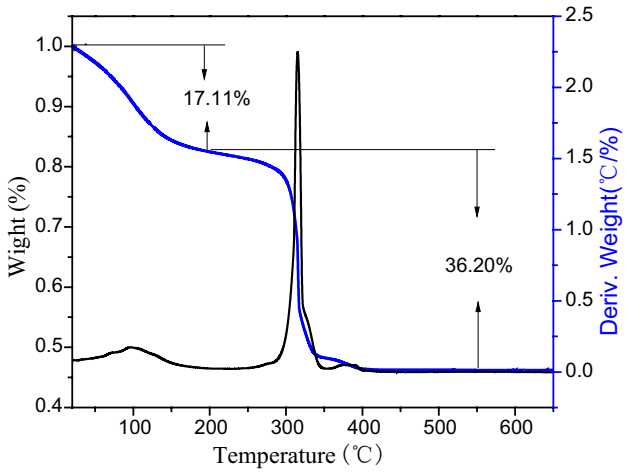

Fig. 3 TGA curve of the cerium pyrazine-2,3,5,6-tetracarboxylate sample

materials have unknown structures [21, 22]. And even some amorphous and not crystalline MOFs were reported in previous literatures [4, 23]. The intense peaks locating at 10.58°, 13.86°, 28.57° and 35.92° in the XRD pattern of sample indicate the possible formation of a newly organized structure.

To further investigate the crystal structure of the cerium pyrazine-2,3,5,6-tetracarboxylate sample, the thermal gravimetric analysis (TGA) curve was carried on in air. From Fig. 3, it can be seen that the TGA curve exhibits two major stages of rapid weight loss in the temperature range from 30 to 400 °C. The first weight loss stage before 200 °C can be ascribed to the release of the physically absorbed and structured water molecules. The second weight loss from 200 to 400 °C is due to the burnout of the organic molecules. The weight loss in the two stages is measured to be 17.11 and 36.20%, respectively. This result is basically in agreement with the theoretical weight loss of the six water molecules (16.76%) and the organic ligand (39.73%) of assumed structure $Ce_2(pztc)(H_2O)_6$. The final decomposition product can be presumed to cerium oxide (CeO_2), thus weight loss in the first and second steps were ascribed to [$Ce_2(pztc)(H_2O)_6 \rightarrow CeO_2 + H_2O + CO_2$]. Moreover, elemental analysis was used to study the composition of the as-obtained products. The experimental contents of C, N, and H are shown to be 15.83, 4.97, and 1.88%, respectively, which are basically in agreement with theoretical value of C (14.90%), N (4.34%) and H (1.86%), confirming the molecular formula of the cerium MOFs is $Ce_2(pztc)(H_2O)_6$.

3.2 Morphology analysis of Ce-MOFs

The morphology of the cerium pyrazine-2,3,5,6-tetracarboxylate architectures were studied using scanning electron microscopy (SEM). Figure 4a shows the overview image of the samples. It can be clearly seen that the products are composed of a large quantity of uniform and beautiful 3D flower-like architectures. From the enlarged SEM image (Fig. 4b), it can be seen that the cerium pyrazine-2,3,5,6-tetracarboxylate flowers with diameter of about 4 μm have some petals and a central nucleus. Interestingly, a more careful observation of a typical flower-like architecture (shown in Fig. 4c) reveal that these flower structures are composed of numerous nanosheets with smooth surface arranging radially from the center of the flower structures with ellips-like shape. In addition, this as-obtained Ce-based MOFs samples could not be destroyed and broken into discrete individual nanosheets even by ultrasonically treating their aqueous suspension for several minutes, indicating that the 3D architectures are not a random aggregate but the ordered self-assembly of the nanosheets. The EDX spectrum of the products (Fig. 4d) shows the presence of Ce, C, O and N (Au from SEM measurement), which agrees well with the above composition analysis.

3.3 Formation mechanism of Ce-MOFs

In order to understand the growth mechanism of cerium pyrazine-2,3,5,6-tetracarboxylate, time-dependent experiments were carried out. The morphological evolutions of the intermediate products collected after different reaction times (1–48 h) were recorded by SEM (Fig. 5). Interestingly, the Ce-based MOFs have formed as little nanosheets and submicron sheets with different sizes after hydrothermal treatment for 1 h (Fig. 5a). With increasing the reaction time to 3 h (Fig. 5b), the number of the sheet-like samples increased and some flower-like particles appeared. After 6 h of hydrothermal treatment, some flower-like particles

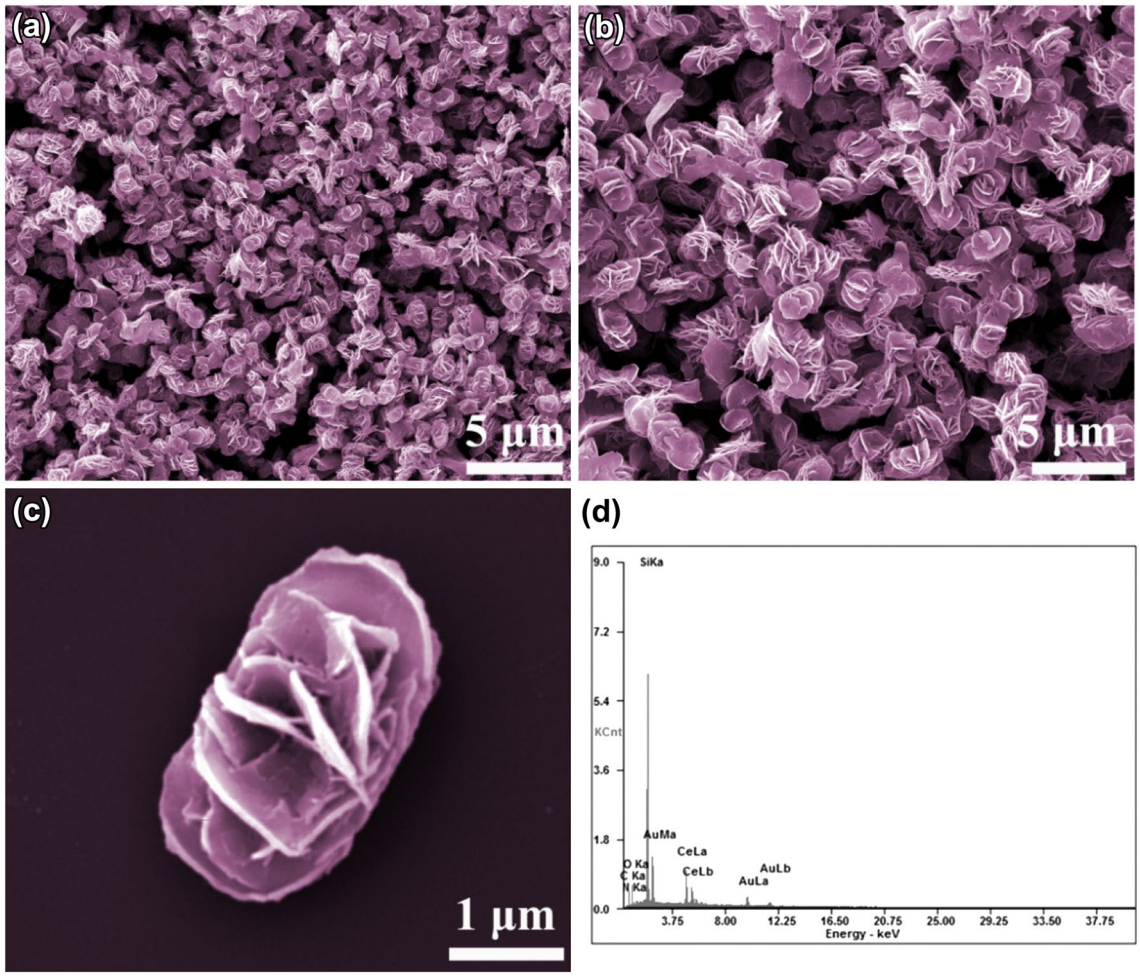

Fig. 4 SEM images of cerium pyrazine-2,3,5,6-tetracarboxylate at different magnification (**a**–**c**), and EDX spectrum (**d**)

increased, as shown in Fig. 5c. By increasing the reaction time to 12 h, the intermediate submicron sheets formed in the front stage disappeared and flower-like samples were obtained with the size about 2 μm (Fig. 5d). When the reaction time increased to 18 h, almost uniform hierarchical flower-like samples were obtained. Moreover, the size of the samples is increased to about 3 μm (Fig. 5e). As the reaction time increased to 24 h, the as-obtained products are composed of a large quantity of uniform 3D flower-like architectures, the size of the samples increase to 4 μm (Fig. 4). Further increasing the reaction time to 48 h, the size of the 3D microflowers increased slightly (Fig. 5f). This result is similar to the sample prepared for 24 h, indicating that the 3D flower-like cerium pyrazine-2,3,5,6-tetracarboxylate samples can be obtained and maintained the morphology when the reaction time exceeds 18 h.

Generally speaking, the growth process of crystals can be classified into two steps: an initial nucleating stage and a crystal growth stage. At the initial nucleation stage, the formation of the seeds is crucial for further growth of the crystals. The subsequent crystal growth stage is a kinetically and thermodynamically controlled process. In our experiments, the Ce^{3+} ions in the solution quickly reacted with ligand anions nucleation to form cerium-MOFs crystal nucleus due to the strong coordination of Ce^{3+} with pyrazine-2,3,5,6-tetracarboxylate at the initial stage of reaction. Under the hydrothermal conditions, each nucleus would quickly grow into nano/submicro-sized sheet. As time goes on, more and more nanosheets would attach to each other to lower their surface energy and assemble to form flower-like structure by Van der Waals attraction [24]. On the basis of the above results, a schematic illustration for the formation of cerium pyrazine-2,3,5,6-tetracarboxylate architectures is presented in Fig. 6. This facile, mild and cost-effective growth strategy may serve as guidance for the synthesis of other nano/micro metal–organic materials with uniform and novel morphologies.

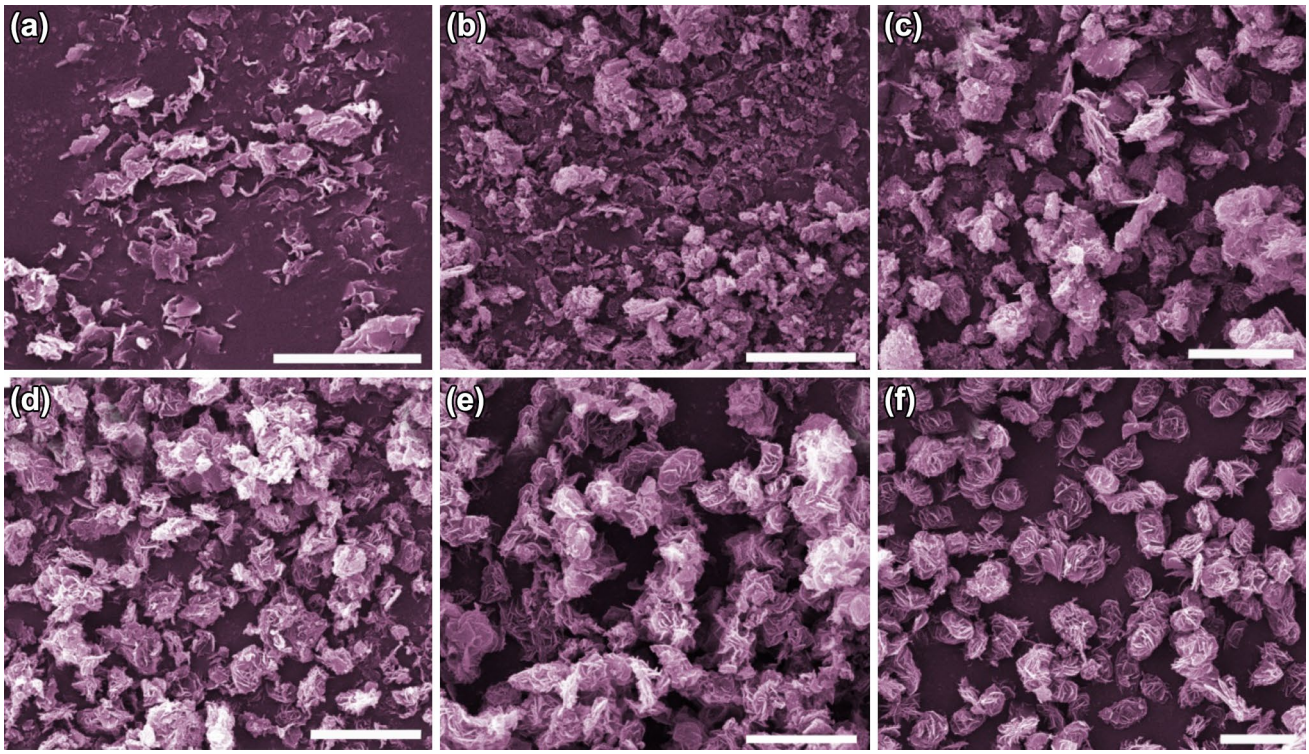

Fig. 5 SEM images of cerium pyrazine-2,3,5,6-tetracarboxylate synthesized with different reaction time: **a** 1 h; **b** 3 h; **c** 6 h; **d** 12 h; **e** 18 h; **f** 48 h (*scale bar* 5 μm)

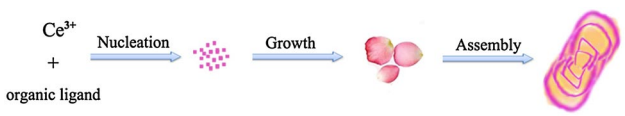

Fig. 6 A schematic illustration for the formation of the cerium pyrazine-2,3,5,6-tetracarboxylate architectures

3.4 Morphology and structure of ceria obtained from calcination of Ce-MOFs

As mentioned in previous section, cerium pyrazine-2,3,5,6-tetracarboxylate architectures could be decomposed by heat-treating process. Figure 7 presents the typical

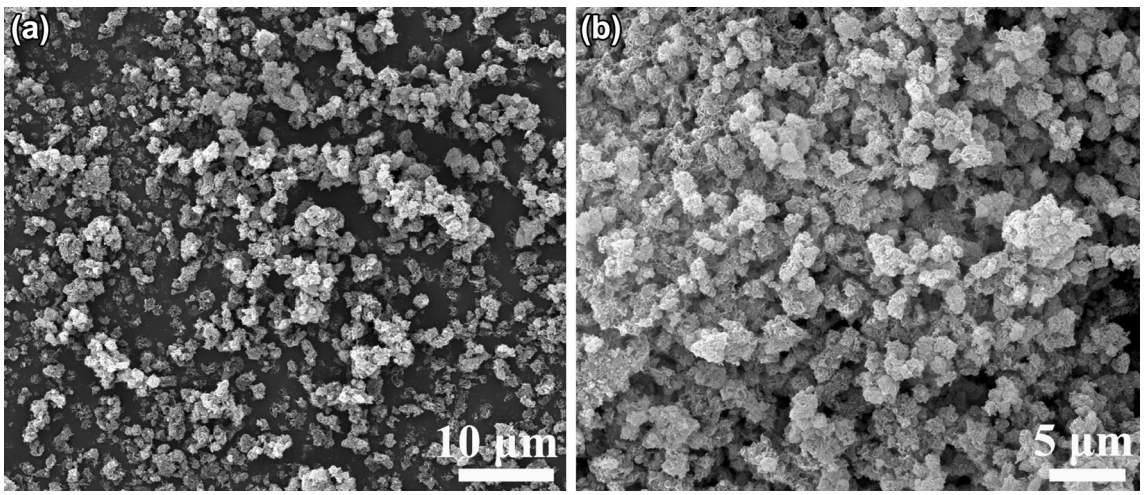

Fig. 7 SEM images of CeO_2 obtained after calcination of Ce-MOFs samples in air at 400 °C

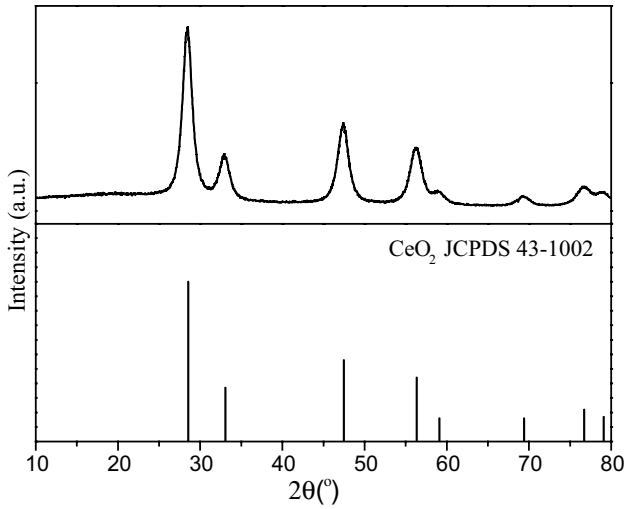

Fig. 8 XRD pattern of the as-obtained CeO_2 and the standard data of CeO_2 (JCPDS NO. 43-1002) as a reference

morphologies of the as-obtained CeO_2 obtained after calcination of Ce-MOFs samples in air at 400 °C. It can be seen that the 3D flower-like crystal is maintained in great part during the solid-state transformation. Nevertheless, the size of the final product decreased to about 2–3 μm and the nanosheets aggregated, which can be ascribed to the dehydration and decarboxylation of the Ce-MOFs during the heating process. Figure 8 shows the XRD pattern of the calcinations products. All the strong and sharp diffraction peaks can be well-indexed to the pure cubic face-centered phase of CeO_2 (JCPDS NO. 43-1002) and no impurity peaks are observed. It indicates that flower-like Ce-MOFs microstructures can be completely transformed into pure CeO_2 microstructures with flower-like outlines through simple heat-treating in air.

4 Conclusion

In summary, through an efficient and one-step approach, cerium pyrazine-2,3,5,6-tetracarboxylate MOFs with uniform 3D flower-like architectures have been successfully prepared through a hydrothermal method. These 3D flower-like architectures with diameter of about 4 μm are composed of a large amount of nanosheets which are assembled in a radial form from the center to the surface. The presumed molecular formula of the cerium MOFs is $Ce_2(pztc)(H_2O)_6$. In addition, time-dependent experiments were carried out. A possible mechanism for the formation of cerium pyrazine-2,3,5,6-tetracarboxylate architectures was proposed. Moreover, interestingly, these 3D flower-like Ce-MOFs samples turn into shape-preserved CeO_2 during the solid-state transformation, suggesting a potential approach for fabricating 3D inorganic materials form metal–organic framework precursors.

Acknowledgements This work is financially supported by the project of Education Department of Sichuan Province (14ZB0026), the Science Research Fund of Sichuan Normal University (DJ2016-34) and the Opening Laboratory Project of Sichuan Normal University (KFSY2016-29).

References

1. K. Liu, H.P. You, Y.H. Zheng, G. Jia, L.H. Zhang, Y.J. Huang, M. Yang, Y.H. Song, H.J. Zhang, CrystEngComm **11**, 2622 (2009)
2. J. Thirumalai, R. Krishnan, I.B. Shameem Banu, R. Chandramohan, J. Mater. Sci.: Mater. Electron. **24**, 253 (2013)
3. Y. Zheng, X. Sun, H. Su, L. Sun, Q. Lin, C. Qi, Inorg. Chem. Commun. **60**, 119 (2015)
4. M. Shi, C. Zeng, L. Wang, Z. Nie, Y. Zhao, S. Zhong, New J. Chem. **39**, 2973 (2015)
5. K. Liu, H.P. You, G. Jia, Y.H. Zheng, Y.J. Huang, Y.H. Song, M. Yang, L.H. Zhang, H.J. Zhang, Cryst. Growth Des. **10**, 790 (2010)
6. X. Zhu, H. Zheng, X. Wei, Z. Lin, L. Guo, B. Qiu, G. Chen, Chem. Commun. **49**, 1276 (2013)
7. D. Chandra, A. Dutta, A. Bhaumik, Eur. J. Inorg. Chem. **2009**, 4062 (2009)
8. J. Puigmartí-Luis, M. Rubio-Martínez, U. Hartfelder, I. Imaz, D. Maspoch, P.S. Dittrich, J. Am. Chem. Soc. **133**, 4216 (2011)
9. B. Liu, M. Chen, C. Nakamura, J. Miyake, D.J. Qian, New J. Chem. **31**, 1007 (2007)
10. B. Zhang, L. Chen, X. Yang, T. Xu, T. Sun, L. Wang, Q. Zhang, J. Mater. Sci.: Mater. Electron. **28**, 7326 (2017)
11. K. Liu, Z.R. Shen, Y. Li, S.D. Han, T.L. Hu, D.S. Zhang, X.H. Bu, W.J. Ruan, Sci. Rep. **4**, 6023 (2014)
12. M. Ranjbar, M.A. Taher, A. Sam, J. Mater. Sci.: Mater. Electron. **27**, 1449 (2016)
13. I.Y.A. Gural'skiy, G. Molnár, I.O. Fritsky, L. Salmon, A. Bousseksou, Polyhedron **38**, 245 (2012)
14. Y. Tang, H.T. Wang, M. Chen, D.J. Qian, L. Zhang, M. Liu, Nanoscale Res. Lett. **9**, 488 (2014)
15. Y. Yang, Q. Hu, Q. Zhang, K. Jiang, W. Lin, Y. Yang, Y. Cui, G. Qian, Mol. Pharm. **13**, 2782 (2016)
16. S. Duan, J. Li, X. Liu, Y. Wang, S. Zeng, D. Shao, T. Hayat, ACS Sustain. Chem. Eng. **4**, 3368 (2016)
17. Z. Ning, H. Wang, W. Li, C. Sun, D. Gao, Chem. Lett. **45**, 229 (2016)
18. Z. Ning, W. Li, Z. Chang, D. Gao, J. Bi, Mater. Res. Bull. **83**, 302 (2016)
19. A.H. Yang, H. Zhang, P. Yin, H.L. Gao, J.Z. Cui, B. Ding, Inorg. Chem. Commun. **13**, 1304 (2010)
20. K. Liu, H.P. You, G. Jia, Y.H. Zheng, Y.H. Song, M. Yang, Y.J. Huang, H.J. Zhang, Cryst. Growth Des. **9**, 3519 (2009)
21. I. Lee, S. Choi, H.J. Lee, M. Oh, Cryst. Growth Des. **15**, 5169 (2015)
22. S. Zhong, M. Wang, L. Wang, Y. Li, H.M. Noh, J.H. Jeong, CrystEngComm **16**, 231 (2014)
23. Y. Huang, B. Liu, Q. Shen, X. Zhu, Y. Hao, Z. Chang, F. Xu, P. Qu, M. Xu, Talanta **164**, 427 (2017)
24. C.M. Zhang, Z.Y. Cheng, P.P. Yang, Z.H. Xu, C. Peng, G.G. Li, J. Lin, Langmuir **25**, 13591 (2009)